HU YAJIE
and
YE JIAREN

Analysis of imaging logging in Ordovician carbonate formation

The reservoir space types of the Tahe oilfield are various and unevenly distributed with strong heterogeneity, which contain Karst holes, cracks and caves. They also make reserving and penetrating mechanisms and reservoir characteristics complicated. Through a brief analysis of the several kinds of imaging logging data applied in carbonate reservoir evaluation in Tahe oilfield, this paper focus on features of the fractured, dissolved pore and karst cave reservoirs recognized by such data with a comparative analysis. By electric imaging logging data, little difference is found among evaluation of different types of reservoirs and FMI borehole coverage and image quality are relatively high; with acoustic imaging logging data, the borehole coverage is higher, thus, it can give a better evaluation of different types of reservoirs in viscous oil area, however, the resolution is lower, for which, it cannot be used in evaluation of corrosion and dissolved pore reservoir.

Key words: Carbonate rocks, acoustic imaging logging, electric imaging logging; dipole acoustic logging.

1. Introduction

Tahe oilfield is located in southwest of the Akekule Arch in Xayar Uplift in Tarim Basin of Xinjiang with the major oil reservoirs of the Ordovician carbonate fracture-cave reservoirs [1-4]. The distinctive features of such reservoirs include reservoir space of fracture, dissolved pore and cavity system, second, oil and gas distribution controlled by karst cave and fracture, strong vertical and lateral heterogeneity, great buried depth (beneath5,300m), thus, exploration and development of the reservoirs is a difficult problem for the whole world [5-6].

Given that logging information is the comprehensive response to lithology, physical property, type of pore and cave, property of the fluid contained of the reservoir, complicated storage and permeability mechanism result in multiplicity of solution, ambiguity and uncertainty of logging reservoir evaluation, for which, conventional logging techniques and means of explanation can only provide a poor evaluation of such reservoir due to limitations of measuring resolution[7]. On this ground, new imaging logging techniques (FMI, DSI, XMAC, MDT, ARI, CMR, MRIL, ECS and ATI) involving advanced technologies with more geological information collected and better evaluation of carbonate reservoir are the main approaches to solve the problem of evaluation of such complex carbonate reservoir [8].

2. Application example of acoustic imaging

Ultrasonic imaging logger can scan the well with a rotary ultrasonic transducer and record the echo waveform signal [9]. The high-resolution image of the whole borehole walls is obtained through 360-degree imaging degree of the scan results after a series of processing of the information measured such as amplitude and propagation time of the echo[10]. The main functions are: (1) realize 360-degree high-resolution caliper logging, through which we can analyze the geometrical shape of the borehole and estimate direction of the crustal stress; (2) detect fracture and evaluate borehole collapse; (3) determine strata thickness and dip angle; (4) analyze shape of strata and sedimentary structure; (5) check
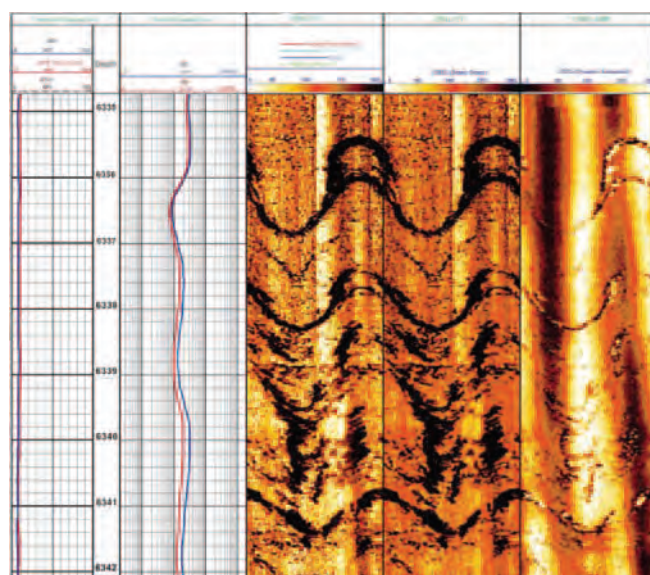

Fig.1 Characteristics of well fractured reservoir

Messrs. Hu Yajie and Ye Jiaren, Faculty of Earth Resources of China University of Geosciences (Wuhan), Wuhan 430 074, Hubei. Mr. Hu is also with Engineering Technology Institute of Sinopec Northwest Oilfield Branch, Urumqi 830 011, Xinjiang, China

the casing for corrosion and deformation; (6) conduct evaluation of the cement bond quality. The imaging loggers currently used in the work ares are: acoustic imaging logger CAST-V and the ultrasonic circumferential borehole imaging logger (CBIL).
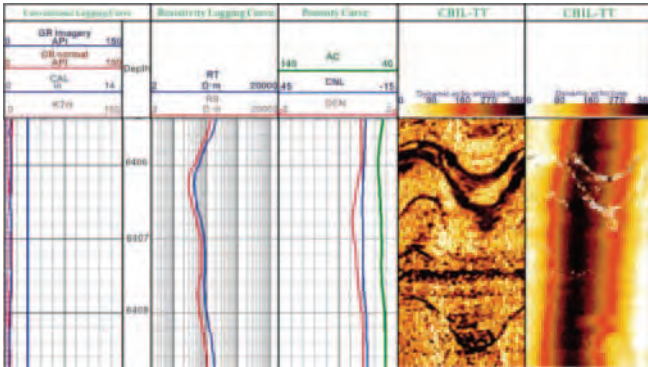

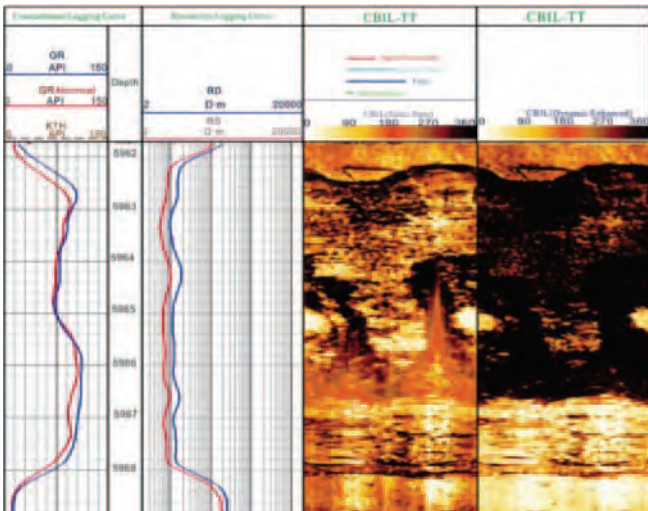Fig.2 Acoustic imaging characteristics of well A2

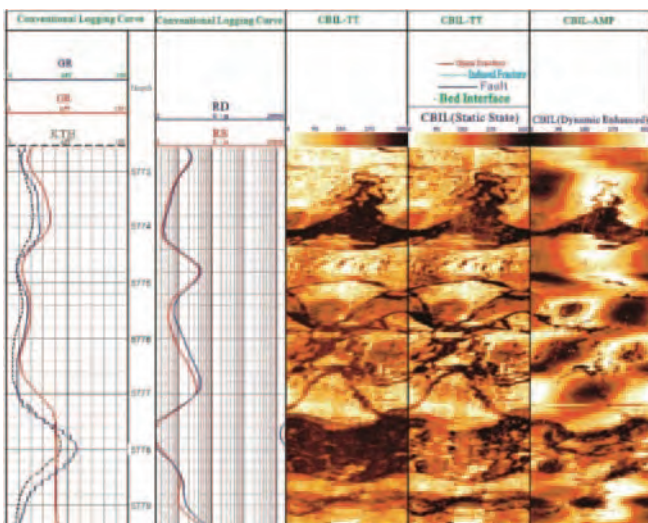Fig.3 Acoustic imaging characteristics of well A3
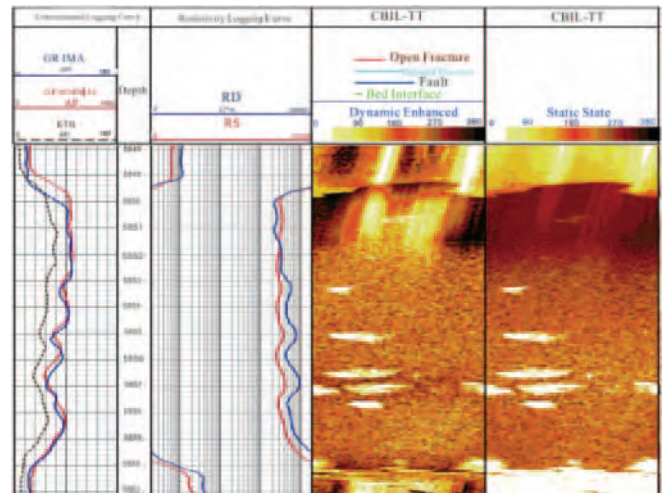

Fig.4 Acoustic imaging characteristics of well A4

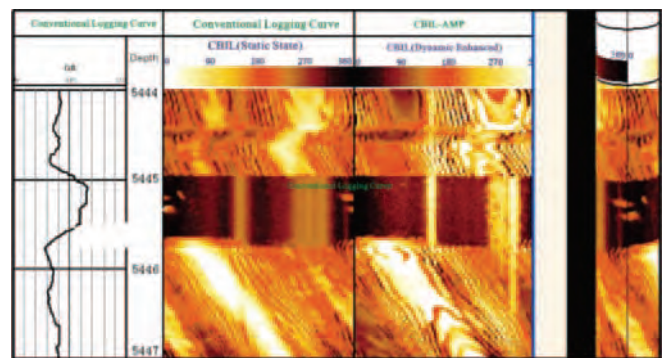Fig.5 Acoustic imaging characteristics of well A5

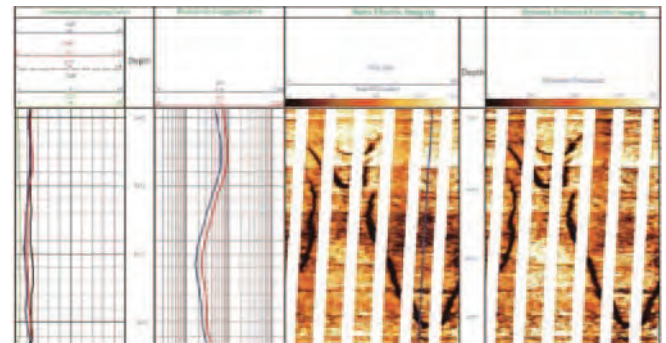Fig.6 Casting detection of well A6

Fig.7 EMI image of well A7

3. Application example of electric imaging

EMI logger is provided with 6 independent measuring arms in its probe, and 2 rows of button electrode system (25 arrays), totalling 150 button electrodes are installed on the plate of each measuring arm. The button electrode is in a diameter of 0.16in (1in=2.54cm) with a distance of 0.2 in between 2 button electrodes in the same row, and a distance of 0.3 in between two rows of button electrodes. It can be seen that the two rows of button electrodes are well-arranged. Thus, the instrument can be used in logging operation of borehole with

the diameter greater than 6 in. With the unique design of EMI logger, we can achieve ideal borehole coverage, which is above 82% in boreholes with the diameter of 6 in. Changes of the micro-resistivity curve recorded by EMI mainly reflect the influence of lithology, fracture, stratification, and karst cave and other stratigraphic characteristics. Variation of colour of the image recorded by the logger, electrical resistivity is indicated but not the actual rock colour in the stratum. A visualized and correct representation of stratigraphic characteristics is given by the features of the images.

4. Application example of dipole shear wave

Dipole shear imaging logging (DSI) is the new generation of full-wave logging after long-spaced acoustic logging. Compared to long-spaced acoustic logging, DSI is provided with more probes, smaller distance, lower frequency of sound wave and better detection of formation shear wave information and record of stoneley wave. Through DSI, we can acquire formation longitudinal wave, shear wave and stoneley wave information, with which, identify lithology and gas layer, determine effectiveness and extension direction of fracture and obtain a large number of rock physical parameters and engineering mechanics parameters.
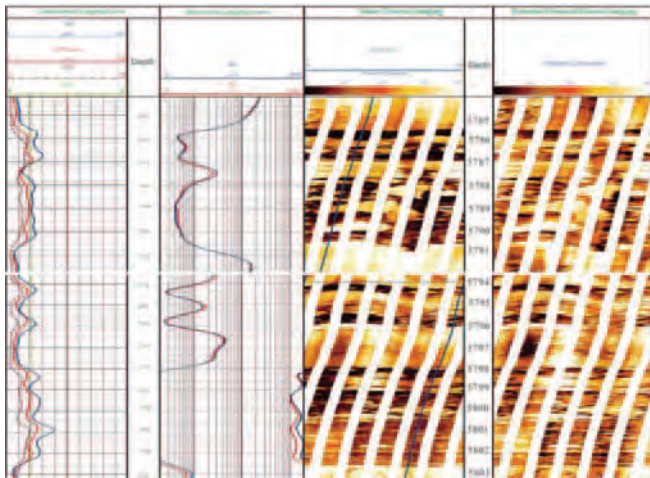

Fig.8 EMI Image of well A8

1. IDENTIFICATION OF LITHOLOGY AND GAS ZONE

The time difference of longitudinal wave and shear wave are obtained by DSI, from which, the p-wave and s-wave velocity ratio is calculated, which is used for identification of lithology.

If there is gas in the pore, the velocity of longitudinal wave decreases significantly but the shear wave is mainly propagated along the rock matrix and has little to do with property of the fluid in the pore. Therefore, under certain rock porosity, with the increase of gas saturation, VP/VS decreases. For this reason, the p-wave and s-wave velocity ratio can be used for division of gas layer.
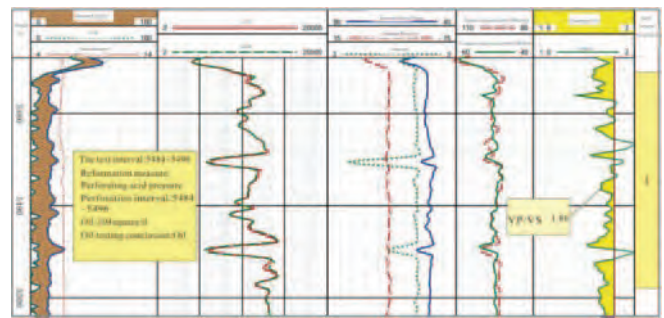

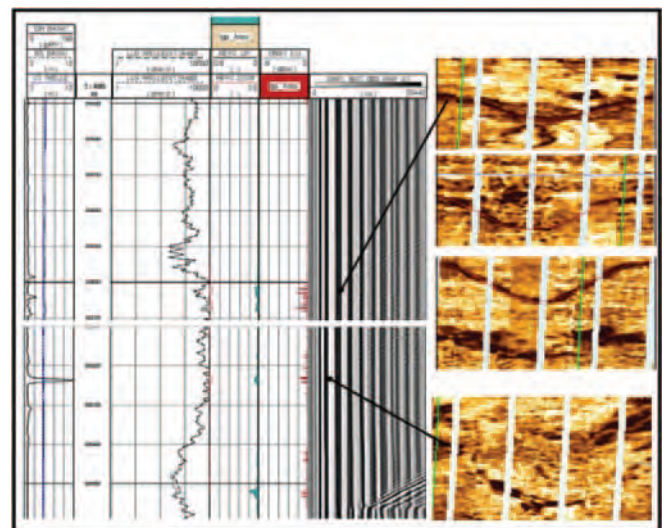Fig.9 Determination of oil and gas layer in well A9 by P-wave and S-wave velocity ratio

Fig.10 Analysis chart of DSI Stoneley wave differential energy and reflection of well A10

2. DETERMINATION OF FRACTURE-DEVELOPING WELL SECTION AND FRACTURE EFFECTIVENESS

Fractures can be recognized by the stoneley wave reflection results and by longitudinal wave, and shear wave and stoneley wave energy attenuation, the fracture effectiveness can be determined. For fracture-developing well section, v type or X ripples are seen in the result map of stoneley wave reflection, and according to the reflection coefficients of the upward and downward stoneley wave obtained by wave-field separation, we can calculate the width of the fracture.

Amplitude attenuation of the longitudinal wave, and shear wave and stoneley wave is related to materials filling the fracture. When the fracture is filled by fluid, the fluid filled will lead to a remarkable decrease of the radial wave impedance value of the formation, and in this case, energy reduction of eight receivers is shown in the energy attenuation result map with the extent in direct proportion to fracture width. Generally, energy reduction of longitudinal wave, shear wave and stoneley wave reflects low-angle fracture development, medium and high-angle fracture development, and good effectiveness of the fracture respectively.

TABLE 1: THEORETICAL VALUES OF P-WAVE AND S-WAVE TIME DIFFERENCE RATIO IN COMMON LITHOLOGY

Lithology	P-wave and S-wave velocity ratio (VP/VS)
Sandstone	1.60
Limestone	1.90
Dolomite	1.80

3. ANALYSIS OF FORMATION ANISOTROPY

Dipole acoustic logging data can analyze the rock mechanical properties and borehole stability, and calculate Poisson ratio, Young's modulus, shear modulus, formation breakdown pressure and sanding index and other parameters. Those parameters can provide reliable basis for calculation of hydraulic fracturing height, gas pressure difference in sanding, perforation stability and borehole collapse in logging, the fracture system.

4. CALCULATION OF ROCK MECHANICS PARAMETERS

With dipole acoustic data and conventional logging data, we can analyze the rock mechanical properties and borehole stability, and calculate Poisson ratio, Young's modulus, shear modulus, formation breakdown pressure and sanding index and other parameters. Those parameters can provide reliable basis for calculation of hydraulic fracturing height, gas pressure difference in sanding, perforation stability and borehole collapse in logging.

5. Electric imaging applications examples

Formation of micro-resistivity scanning imaging logger is provided with several small button electrodes with small distance in many polar plates. When the electrode is buttoned up to the borehole wall stratum for current emission, the difference in electrical conductivity of rock constituent, structure and the rolling body contained in the rock in contact with the electrode will trigger variation in the current, according to which, we can obtain the borehole wall image of resistivity.

1. VERTICAL WELL

In combination with the actual coring data in the research area, 8 images suitable for recognition of different types of carbonate reservoirs in Tahe oilfield are established, including 5 special reservoir models: (1) formation of interface (such as lamina surface, laminaset interface, surface and surface of unconformity), (2) fault, (3) basic bedding types (such as horizontal bedding, parallel bedding and cross bedding etc.), (4) special sedimentary structure (such as slump structure and load structure etc.), (5) gravel and breccia (gravel diameter>1cm); and 3 common reservoir models: (6) dissolved pore, (7) fracture (Low-resistance filled fracture, high-resistance filled fracture, straight-splitting fracture, conjugate joint, pinnate induced joint, and standing induced joint), (8) unfilled, semi-filled and filled karst cave etc.

2. HORIZONTAL WELL

For horizontal well, the geological phenomena easily to be recognized by FMI imaging logging data are: fracture, karst cave, dissolved pore, siliceous lump, and filled fracture. In order to acquire a clear understanding of the response characteristics of FMI imaging logging of horizontal well, it is necessary to carry out a comparative analysis of the corresponding geological phenomena in vertical well.
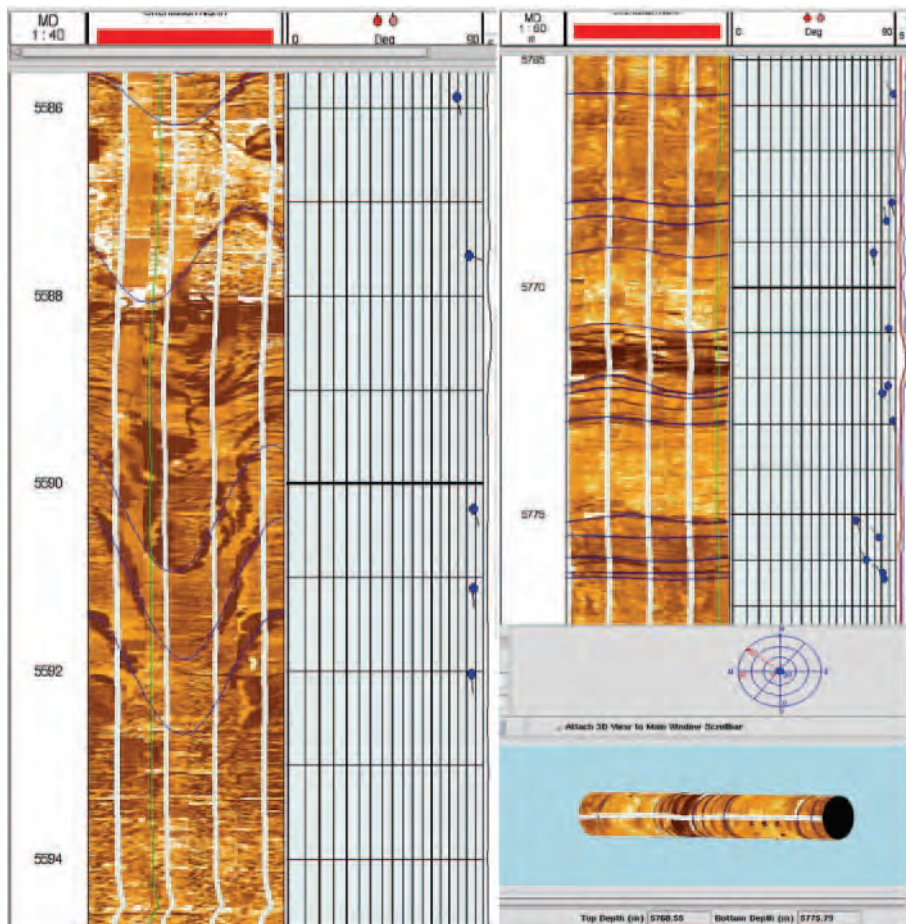

Fig.11a.   Fig.11b.

Fig.11a: Fracture in vertical well A11, high dip angle (80°-90°). Fig.11b: Fracture with high-dip angle (true dip angle of 80°-90° at various occurrences in horizontal well, but the apparent dip is very low because the borehole runs across the fracture strike in horizontal logging (B1, 5,768-5,775 meters)

Fig.12a Both the apparent and true dip of chert nodule and chert banding distributed along the formation are very low in vertical well (well A12)
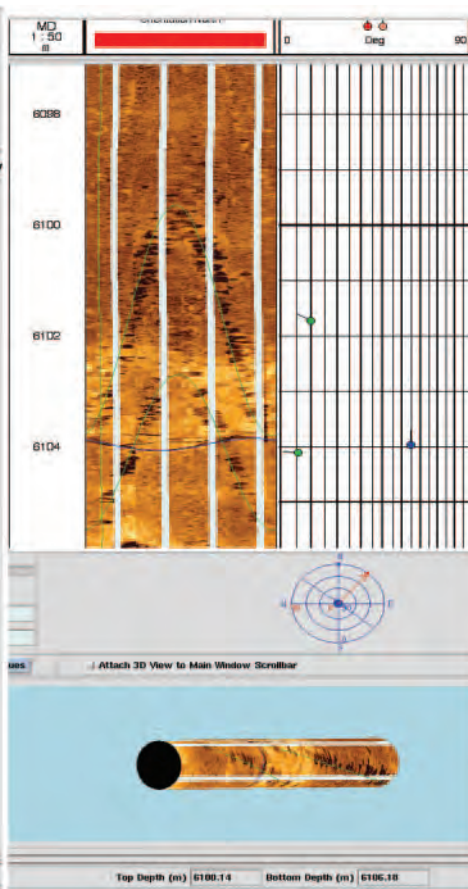
Fig.12b The chert nodule and chert banding distributed along the formation is of an apparent dip much higher than the true dip (B2, 6,100-6,105 meters)

1. Fracture

In vertical well, the fracture is mainly high-angle fracture (60º-90º) with certain difference in the direction of tendency (or the strike) caused by structural position and formation phase of the fracture. Besides, because the borehole nearly runs across the formation horizontally, the fracture detected by FMI imaging logging in such occurrence is in an apparent dip lower than the true dip. The fracture filled by calcite is of the same characteristics with the unfilled fracture except that is shown by brighter sine curves in the imaging logging data of both vertical and horizontal well.

2. Siliceous lump

For vertical well, siliceous lumps are represented by wide black stripes or long ovals easily to be recognized in the imaging logging data. However, in conventional logging data, conventional logging response of the siliceous lump development section is very similar to that of the fracture development section. In horizontal well imaging logging data, because the horizontal borehole runs across the formation horizontally, the chert nodule and chert banding distributed along the formation is of an apparent dip much higher than the true dip.

3. Karst cave

Karst cave is easily to recognize in imaging data, if the cave is filled by sandstone, there must be some bright colours in the dynamic image for imaging logging that are darker than the limestone. If the cave is filled by mud, the colours are darker than sandstone. The difference of the karst cave in horizontal well and vertical well does not lie in the karst cave section itself but the periphery of the cave. In general, there are a few NW tendency and SE tendency dissolution fractures above or below the karst cave in vertical well, but there are more NW tendency and SE tendency dissolution fractures above or below (actually at the left and right sides) the karst cave in vertical well.

6. Comparative analysis of different types of imaging logging data

In micro-resistivity imaging logging, the number of button electrodes provided by FMI instrument and borehole coverage are obviously greater than that of the EMI and STAR series. For 6" borehole, FMI coverage is about 95%, while the EMI coverage is about 82%. The overall image quality and instrument stability of FMI is better than that of EMI and STAR, but FMI logging requires a higher cost.
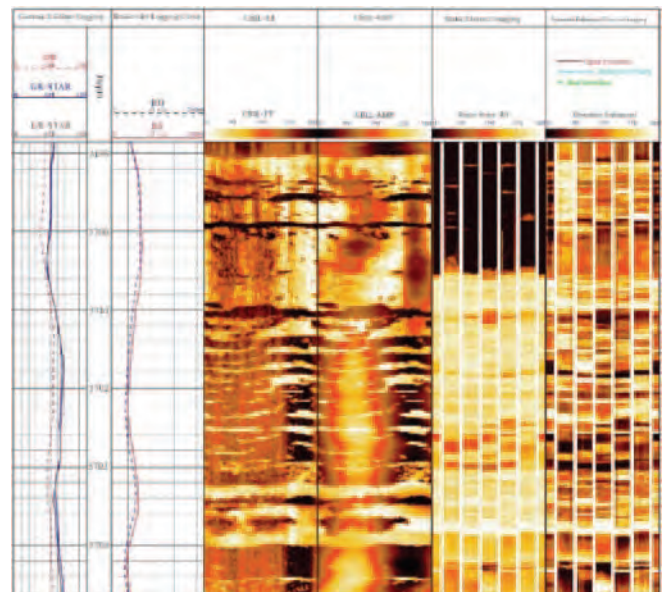

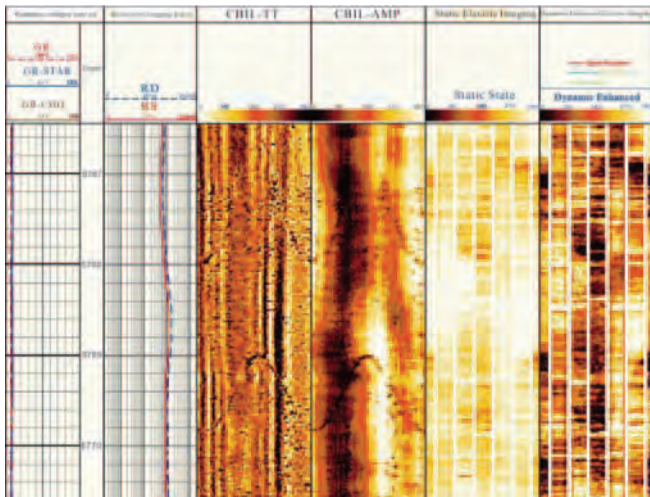Fig.13 Acoustic imaging characteristic of well A15

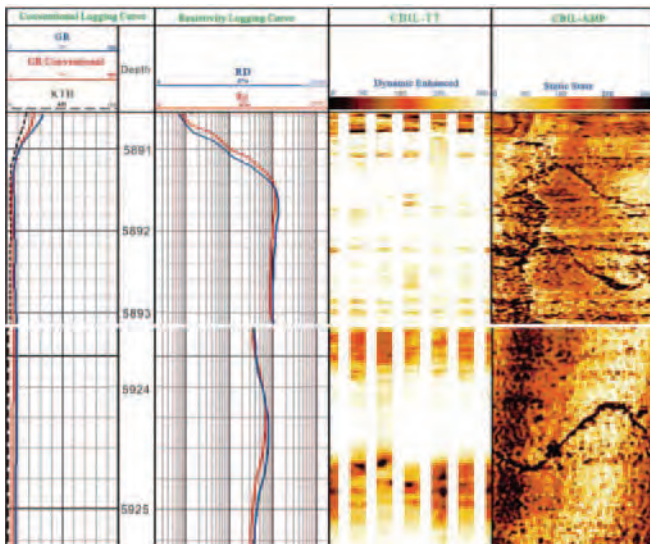Fig.14 Acoustic imaging characteristic of well A16
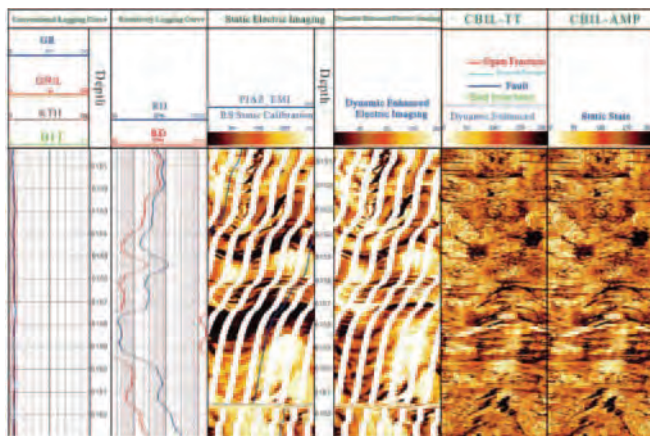

Fig.15 Acoustic imaging characteristic of well A17

Fig.16 EMI and acoustic image of well A18

Compared to the electrical imaging logging data, acoustic imaging logging can provide a relatively larger coverage but a significantly poorer measurement precision.

Given that fractured reservoirs in Ordovician viscous oil area of Tahe oilfield are prone to be filled by heavy oil, it is hard to recognize those reservoirs by conventional logging curves. With the aid of acoustic imaging logging data, we can eliminate the interference from heavy oil and improve logging interpretation of the reservoir and geological analysis.

7. Conclusion

Imaging logging techniques can be applied in formation division, recognition of reservoir type, and determination of reservoir effectiveness in evaluation of Ordovician carbonate reservoir in Tahe oilfield. According to the images obtained by imaging logging, and with man-machine interaction interpretation results, we can determine occurrence and strike of the fault, formation drag structure, unconformity, formation occurrence and change etc. Thus, we substantially improve the ability to evaluate complicated and heterogeneous reservoir and conduct comprehensive geological researches on reservoir thickness and development layer, occurrences and types required by oil- gas exploration.

References

1. Azmy, K.A., Lavoie, D.L. and Knight, I.K., et al. (2008): "Dolomitiztion of the Lower Ordovician Aguathuna Formation carbonates." *Canadian Journal of Earth Sciences*, 45(7), 795-813.
2. Lavoie, D., Ghi, G. and Brennan-Alpert, P., et al. (2008): "Hydrothermal dolomitization in the Lower Ordovician Romaine Formation of the Anticosti Basin: significance for hydrocarbon exploration." *Bulletin of Canadian Petroleum Geology*, 53(53), 454-471.
3. Cañas, F. L. (1999): "Facies and sequences of the Late Cambrian-Early Ordovician carbonates of the Argentine Precordillera: A stratigraphic comparison with Laurentian platforms." *Special Paper of the Geological Society of America*, 133, 43-54.
4. Kim, J.C. and Yong, I.L. (1996): "Marine diagenesis of Lower Ordovician carbonate sediments (Dumugol Formation), Korea: cementation in a calcite sea." *Sedimentary Geology*, 105(3-4), 241-257.
5. Pang, H., Chen, J. and Pang, X., et al. (2013): "Analysis of secondary migration of hydrocarbons in the Ordovician carbonate reservoirs in the Tazhong uplift, Tarim Basin, China," *Aapg Bulletin*, 97(10), 1765-1783.
6. Yuan, L., Zhou, H. and Jing, X., et al. (2014): "Microfacies and Facies Analysis of the Ordovician Carbonates in the South Margin of the Ordos Basin." *Acta Geologica Sinica*, 88(3), 421-432.
7. Voldman, G., Albanesi, G. L. and Ramos, V. A. (2009): "Ordovician metamorphic event in the carbonate platform of the Argentine Precordillera: Implications for the geotectonic evolution of the proto-Andean margin of Gondwana." *Geology*, 37(4), 311-314.
8. Taylor, S. R. and Mclennan, S. M. (1995): "The geochemical evolution of the continental crust." *Reviews of Geophysics*, 33(2), 293-301.
9. Kidwell, S. M. and Brenchley, P. J. (1994): "Patterns in bioclastic accumulation through the Phanerozoic: Changes in input or in destruction." *Geology*, 22(12), 1139-1143.
10. Davis, G. A., Darby, B. J. and Zheng, Y., et al. (2002): "Geometric and temporal evolution of an extensional detachment fault, Hohhot metamorphic core complex, Inner Mongolia, China." *Geology*, 30(11), 1003-1006.